Volume 12, Number 2 (April 2019) p. 398 – 407 • ISSN 1983-4195
http://dx.doi.org/10.1590/S1983-41952019000200011

REVISTA IBRACON DE ESTRUTURAS E MATERIAIS
IBRACON STRUCTURES AND MATERIALS JOURNAL

Effect of temperature gradients on the behaviour of jointed plain concrete pavements

Efeito de gradients de temperatura no comportamiento de pavimentos de concreto com juntas

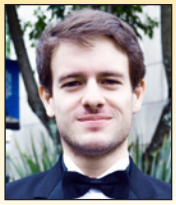

P. B. TRUJILLO [a]
pasquale.basso-trujillo.1@ulaval.ca
https://orcid.org/0000-0002-5914-0214

M. A. S. GUERRERO [b]
In Memorian

Abstract

In many countries of Latin America, Jointed Plain Concrete Pavements (JPCP) are designed using the American Association of State Highway and Transportation Officials (AASHTO) or the Portland Cement Association (PCA) methods, none of which take explicitly into account the environmental conditions of the specific region where a JPCP will be built. It is well known that temperature gradients across the thickness of concrete slabs produce curling which can cause slabs to lose support at its corners and its center depending on the time of the day. This situation, in combination with vehicle loading, generates tensile stresses which can be significant enough to cause initial cracking and the subsequent failure of the pavement. In this research, the Finite Element (FE) package EverFE2.25 was used to study the impact of temperature gradients (calibrated to account for humidity gradients) in combination with a vehicle load (a dual wheel tandem axle of 180 kN) on the performance of a typical JPCP highway section. For the JPCP under study, the apparent increase of the tensile stresses attributable to negative local (ΔT = -18.5°C) Equivalent Temperature Gradients (ETGs) was as 5.5 times larger than the one induced by the axle when it was placed at the border of the slab and up to 8.8 times larger when it was placed at the corner of the slab. Although the apparent increase was not as high when the positive local ETGs (ΔT = +18.5°C) were used, the absolute magnitude of the stresses in combination with the vehicle load were still high enough for the pavement to fail under fatigue. Thus, local temperature gradients should be studied regionally and considered in the design of JPCP using more suitable design procedures such as the Mechanistic-Empirical design procedure.

Keywords: concrete pavement, curling, temperature gradients, finite element analysis.

Resumo

Em muitos países da América Latina os pavimentos de concreto com juntas (JPCP) são calculados usando os métodos da “American Association of State Highway and Transportation Officials (AASHTO) ou da “Portland Cement Association” (PCA), os quais não levam em consideração explicitamente as condições climáticas específicas de cada região onde um JPCP será construído. É muito conhecido o empenamento causado pelos gradientes térmicos que se apresentam através da espessura do pavimento, o qual pode ocasionar a perda de suporte nas extremidades ou no centro da placa dependendo do momento do dia. Esta situação, paralelamente com as cargas veiculares, produzem esforços de tensão que podem ser de suficiente importância para iniciar a fissuração e finalmente a falha completa por fadiga. Nesta investigação, o software de Elemento Finito (EF) EverFe2.25 foi usado para estudar o impacto que os gradientes termicos (calibrado para considerar os gradientes de humidade), em combinação com as cargas veiculares (tandem com duas rodas de 180 kN), tem sobre o comportamento de uma tipica seção de JPCP. Para o JPCP em estudo, o aumento aparente do esforço de tensão atribuído aos Gradientes Térmicos Equivalentes (ETGs) negativos locais (ΔT = -18.5°C) foi 5.5 vezes maior do que os esforços induzidos pelo eixo quando posicionado na borda da placa e até 8.8 vezes maior quando foi colocado o canto da placa. Apesar de que o incremento aparente não foi tão grande quando analisados os ETGs positivos (ΔT = +18.5°C), a amplitude absoluta do esforço calculado nas combinações com as cargas veiculares para estas situações são suficientemente grandes para que ocorra falha por fadiga. Portanto, os gradientes termicos locais tem que ser tomados em consideração para o calculo dos JPCP usando procedimentos de design mais adequados, como o procedimento Empírico-Mecanicista.

Palavras-chave: pavimento rígido, empenamento, gradientes térmicos, análise por elemento finito.

[a] *Faculté de Sciences et Génie, Department of Civil and Water Engineering, Université Laval, Québec, Canada;*
[b] *Facultad de Ingenierías, Departamento de Ingeniería Civil, Universidad Panamericana, Zapopan, México.*

Received: 13 Nov 2017 • Accepted: 14 Jun 2018 • Available Online: 28 Mar 2019

This is an open-access article distributed under the terms of the Creative Commons Attribution License

© 2019 IBRACON

1. Introduction

Jointed Plain Concrete Pavements (JPCP) are typically designed by either (or both) the AASTHO [1] or the PCA [2] methods in many countries of Latin America. The former method was developed based on the information gathered by long-term tests performed on concrete pavements built in Illinois, U.S.A., in 1956 (the AASHO road test) and the latter method by using some of the AASHO road test results in conjunction with results of stresses and deflections of concrete pavements obtained using the FE method. Unfortunately, environmental conditions are only implicitly considered in the AASHTO method of design and are, actually, unaccounted in the PCA method of design. In fact, during the AASHO road test (performed in Ottawa, Illinois), the maximal and minimal temperature gradients measured in the concrete slabs were $\Delta T = +10.2°C$ and $\Delta T = -4.9°C$ in June and July respectively but these values might not be of the same magnitude in other regions of the world with warmer climates.

Temperature gradients, i.e. the temperature difference between the top and the bottom of a slab at a given moment of the day, cause the concrete slabs in JPCP to curl upward or downward during nighttime (negative gradient) and daytime (positive gradient) respectively, resulting in the loss of support at their corners and center. Consequently, the own weight of the slab, in combination with vehicle loads, produce stresses which can exceed the tensile strength of the concrete and cause the slab to fail [3]. Historically, the response of concrete pavements to thermal stresses has been studied assuming a linear distribution of the gradients across the thickness of slabs but it is well known that they are in fact *non-linear* [4-6]. However, considering a *non-linear* distribution underestimates the stresses during daytime and overestimates them during nighttime when computing the response of concrete pavements analytically [3]. Moreover, similar to temperature gradients, humidity gradients can cause an upward and downward warping of the slabs [7-10]. Nonetheless, in most cases the top surface of the slab is partially saturated and its bottom is usually close to saturation, producing an upward warping (negative humidity gradient) almost throughout the entire day [11].

Thus, the use of the AASHTO or the PCA methods is not entirely appropriate in locations where the environmental conditions differ from Ottawa, Illinois. In fact, the most accurate methodology to design a concrete pavement is to gather information regarding local materials, traffic, environment conditions, etc. of the location where the pavement will be constructed and use them to calculate the stresses and deflections of the pavement slabs in order to propose an adequate section thickness. This technique, referred to as the *Mechanistic-Empirical Design Procedure* [1], is currently little employed in many countries of Latin American since it requires, among others, local temperature and humidity gradients of each region which are normally unavailable.

1.1 Research problem and objectives

Since temperature gradients can generate important thermal stresses capable of exceeding the tensile strength of the concrete, the currently used methods of JPCP design should be carefully employed. Instead, the application of a *Mechanistic-Empirical Design Procedure* becomes a better design practice. However, many valuable information for its use, such as the magnitude of temperature gradients, is currently unavailable in many regions and therefore their impact on the behavior of JPCPs cannot be accurately determined. Thus, only an analysis using actual *in-field* data should determine up to what extent their effect, in combination with vehicle loads, is important for the design of concrete pavements in each region. This investigation seeks to establish the significance of considering temperature gradients (calibrated to consider humidity gradients) when designing JPCP by analyzing the stresses induced by local temperature gradients and axle loads over a typical JPCP highway section of the region of Guadalajara, Mexico; the procedure however, can be applied in other regions.

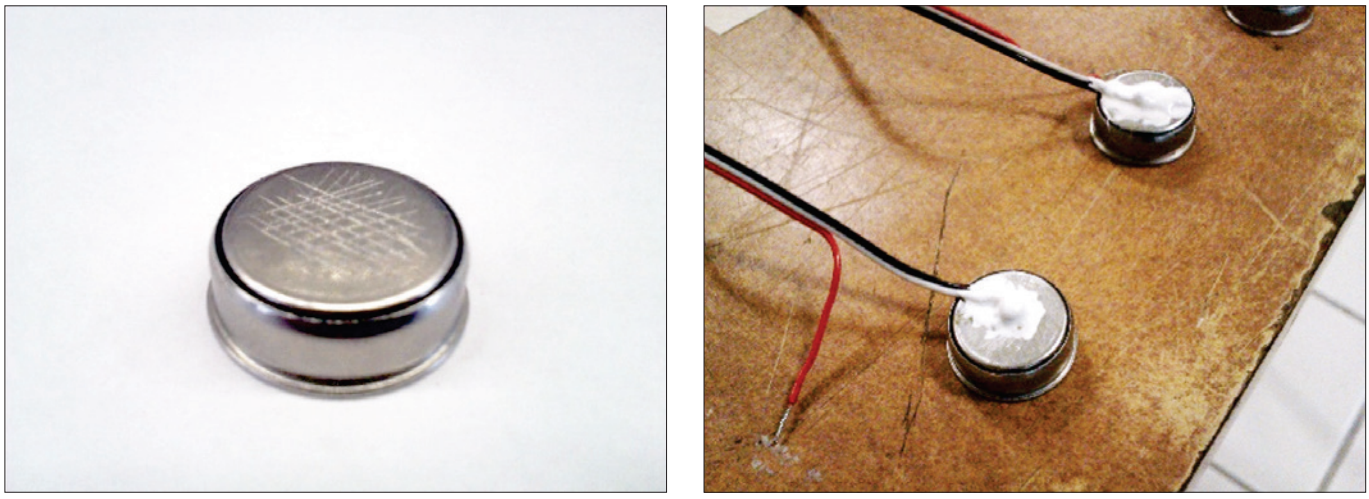

(a) (b)

Figure 1
(a) DS1921-G ibutton and (b) soldered cable over ibutton

2. Methodology

A single concrete slab was built with temperature sensors across its thickness to measure the temperature gradients presented in the hottest season of the city of Guadalajara, México. The vertical displacements of the slab (resulting from combined *built-in* curling, temperature induced curling and humidity induced warping), were also measured *in-field* over two consecutive days. Then, using the *in-field* temperature gradients, the vertical displacements of the slab were calculated with the FE package EverFE2.25 and were compared to the ones measured *in-field*. This allowed to calibrate the temperature gradients to account for the humidity induced warping in accordance with the *in-field* vertical displacements at the most critical moments of the day. Thereafter, the FE package was used to calculate the stresses on a typical JPCP highway section using the calibrated gradients (referred here to as *Equivalent Temperature Gradients* or *ETGs*) in combination with a dual wheel tandem axle.

2.1 Slab construction, instrumentation and monitoring

A 200 mm thick[1] square slab with 4500 mm long sides was constructed[2] over a granular base made with coarse aggregate and river sand. A *plate load* test was performed over the granular base to obtain the modulus of subgrade reaction (*k-value*). Furthermore, the slab was instrumented with temperature sensors (see Figure 1a and 1b) at 3 different locations; center, corner and border. Each location contained 5 equally spaced sensors along the thickness of the slab. They were secured in place by attaching them with plastic tie-wraps to steel threaded rods which were later anchored to the granular base (see Figure 2a). All sensors consisted of DS1921-G ibuttons soldered to cables which were extended outside the slab area so the recorded data could be downloaded to a computer once the slab was cast. The sensors were covered with epoxy to avoid damage from water intrusion; the complete procedure is described in detail in Ref. [12]. In addition, a single unprotected temperature sensor was placed next to the slab in order to record the *in-situ* air temperature. All sensors (inside and next to the slab) were set to record the temperature at a 5 minute interval.

Round steel rods with a square metal plate attached to their top were anchored to the ground close to all four corners of the slab to hold dial gages with a magnet base to measure the vertical displacements of the slab. An additional rod covered with a PVC sleeve (to allow the slab to move freely in the vertical direction) was also anchored to the subgrade at the center of the slab. Concrete of 19 mm (¾ in.) maximal aggregate size with a specified compression strength (f'_c) of 35 MPa was delivered by a concrete mixer and was vibrated using a 1¼ in. head vibrator. Special care was taken when the vibrator was inserted next to the temperature sensors to avoid damaging them. The slab was then screeded and bullfloated (see Figure 2b) and, once the final set was attained, it was finished using a power float. Finally, a water-based curing

(a) (b)

Figure 2
(a) Border ibutton tower and (b) bullfloating of slab

[1] *A mean of 206 mm thickness was calculated based on 28 measurements prior to placing the concrete;*
[2] *Located at 20° 40' 41.5" N 103° 26' 31.5"W.*

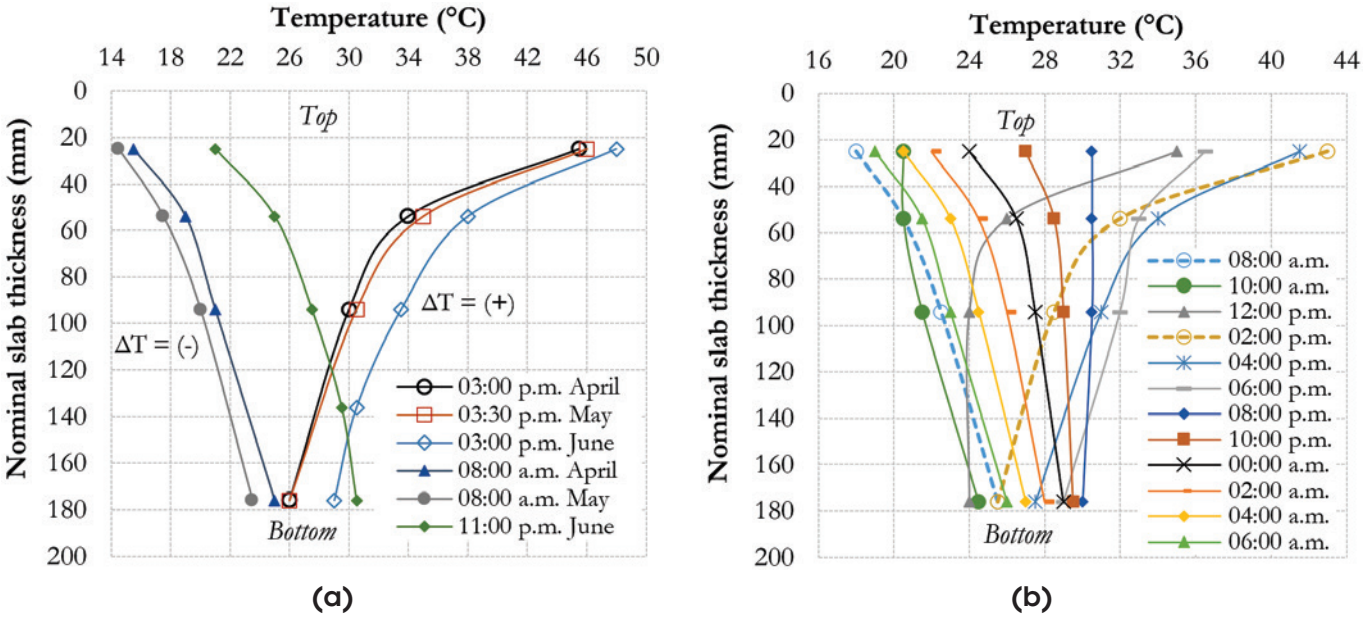

Figure 3
(a) Maximal and minimal monthly temperature gradients and (b) typical hourly variation of the gradients

compound was applied over the slab. The formwork was stripped two weeks later and the sides of the slab were covered with the same curing compound to avoid, as much as possible, any water loss from its sides. Material from the excavation was then used to cover the sides in order to leave its top surface at the same level as the surrounding ground. Temperature readings were recorded from the 6th of April until the 10th of August 2013. Moreover, a 2-day *monitoring period* was undertaken where the vertical displacements of the slab were recorded at its center and four (4) corners using dial gages whose shafts were laid on small square pieces of glass placed over the slab.

3. Results and discussion

3.1 Acquisition of temperature readings

The daily maximal and minimal linear temperature gradients recorded over the entire study ranged between ΔT = +19.0°C to +20.0°C and ΔT = -9.0°C to -9.5°C respectively (refer to Figure 3a for the largest values). Usually, the maximal positive gradients occurred between 2:00 and 4:00 p.m. and the minimal negative ones between 7:00 and 8:00 a.m. However, as the mornings became warmer during the summer, negative gradients occurred late at night (around 11:00 pm) as it was observed in June. When the rainy season started, at mid-June, the absolute magnitude of the gradients started to decrease progressively and are thus not presented here; the detailed information can be found in Ref. [12]. A typical hourly temperature gradient variation (from May 23rd to May 24th 2013) is presented in Figure 3b. For this period of time, the maximal and minimal gradients were ΔT = +17.5°C and -7.5°C respectively (both shown with dotted lines). In general, it can be observed that negative gradients are somewhat more *linear* than positive ones which present a steeper temperature variation within the first 60 mm of the thickness of the slab.

3.2 Monitoring the vertical displacements of the slab

The data recorded during the *monitoring period* (from May 22nd to May 24th 2013) is shown in Figure 4. The center (δ center) is subtracted from the average corner (δ corner) displacements to determine the height difference between both positions, and is represented by the dark dotted line in the same figure. Comparisons needed to be based on this difference since the actual position of the corners and the center of the slab at the moment the *monitoring period* started was unknown. The temperature gradients (ΔT weighted) presented in the same figure by a solid line are preliminarily assumed to vary linearly for the sake of simplicity given the disparity between positive and negative distribution of the gradients (as mentioned previously).

The temperature used to compute the gradients, at both the top and the bottom surface of the slab, represent the weighted temperatures from the center, border and corner of the slab calculated using Equation 1. The weighting coefficients (4, 2 and 1) were subjectively determined based on the amount of slab surface surrounding the towers of temperature sensors, i.e. the border and corner are only surrounded by one-half (½) and one-quarter (¼) of the sides, respectively, in comparison with the center when the slab is imaginarily divided into 4 equal pieces.

$$\Delta T_{weighted} = \frac{4T_{center} + 2T_{border} + T_{corner}}{7}, (°C) \quad (1)$$

From Figure 4, it can be observed that as the peak minimal temperature gradients (negative ΔT weighted) occur, the maximal vertical

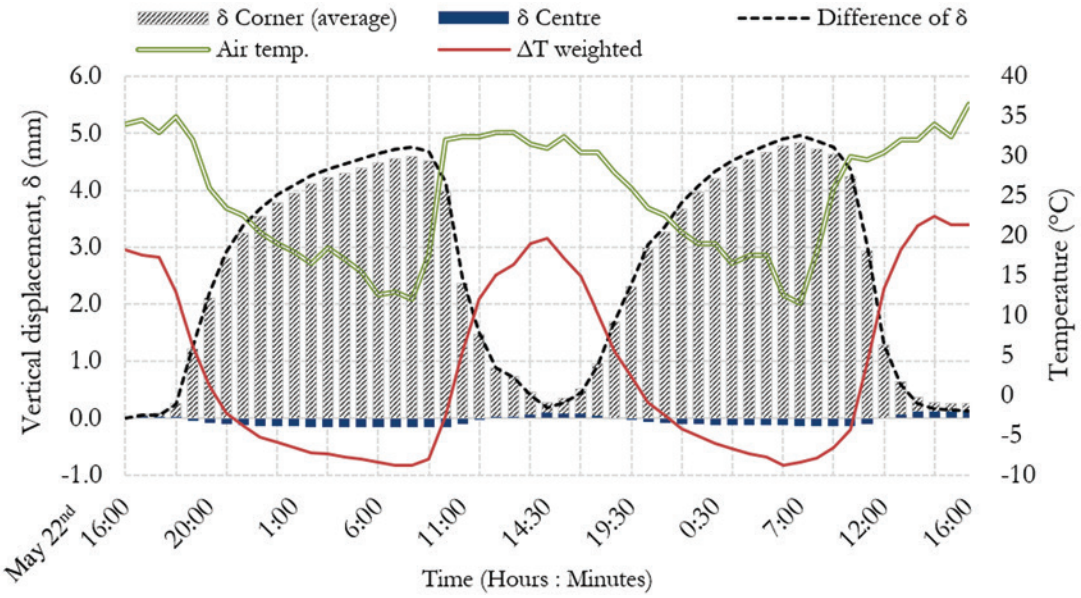

Figure 4
Displacement (δ), gradients (ΔT) and air temperature during the monitoring period

difference between the corner and the center of the slab is reached and *vice versa*. Moreover, at the peak maximal temperature gradient (positive ΔT weighted), the vertical difference remained positive indicating that the corners of the slab were higher than the center at any moment of the day. This can be explained by the fact that the slab suffered from *built-in* curling during construction, i.e. permanent upward curling (refer to Figure 5) of the slab due to the effect of temperature and humidity gradients while the concrete hardened. This may have occurred even with the use of a curing compound because of the hot and windy weather. In addition, Figure 4 shows how the ambient temperature can be a good indicator of the temperature gradients presented across the thickness of the slab.

3.3 Calibration of the temperature gradients intended for FE analysis

In order to verify the adequacy of using the temperature measured in the field as an input for the FE package, the vertical difference between center and corner of the single slab described in section 3.2 was predicted using EverFe2.25. The linear temperature gradients (extrapolated to the top and bottom surface of the slab) measured during the *monitoring period* (May 22nd to May 24th 2013) were used for this purpose. Table 1 summarizes the geometry of the slab used in the model as described in section 2.1.

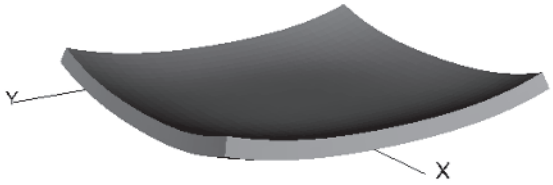

Figure 5
Upward curvature of a single slab

Table 1
Properties of the test slab and the granular base used in EverFE2.25

Category	Parameter	Value
Geometry	Slab length, l x l (mm)	4500 x 4500
	Slab thickness, h (mm)	206
Concrete	Young modulus, E (MPa)	26,500
	Poisson's ratio, ν (-)	0.18
	C. of thermal expansion, α (/°C)	1.0 x 10-5
	Density, γ (kg/m³)	2 300
Base type	Winkler foundation	Tensionless
	k-value (MPa/mm)	0.28
Loading	Thermal gradient	Linear
Meshing	N° elements per slab	30 x 30 x 4

The modulus of elasticity (E) was calculated using Equation 2 [13] with a concrete compressive strength (f_c) of 31.8 MPa at 28 days (obtained from 150 mm diameter cylinders) and the typical density of unreinforced normal weight concrete (γ) of 2300 kg/m^3. The value of E, rounded to the nearest 500 MPa, resulted in 26 500 MPa. The value of the coefficient of thermal expansion of concrete (α) is typically chosen in between 0.9 x 10^{-5} and 1.0 x 10^{-5} [16] so the latter was used for convenience. This value, albeit slightly high, lies within the limits for concretes made with basalt aggregates which are typical of the region. The typical Poisson's ratio (v) of 0.18 was used in the study. The slab was modeled over a Winkler type foundation where unrestrained upward displacements due to curling (only temperature gradients can be introduced in the model) can be considered. A *k-value* equal to 0.28 MPa/mm was calculated based on the second loading cycle from the *plate load* test.

$$E = 0.043\gamma^{1.5}\sqrt{f_c}\ , (\text{MPa}) \quad (2)$$

The vertical displacement difference between the center and the corner of the slab obtained with EverFe2.25 are shown in Figure 6 in comparison with the displacements values computed from the field measurements. It can be observed that the prediction is relatively accurate during daytime, but at nighttime, the prediction significantly underestimates the actual vertical displacement difference. Although it is difficult to explain the exact reason for this difference, a possible explanation might be the presence of humidity gradients across the thickness of the slab which were no considered when the vertical displacements were calculated using EverFE2.25. Indeed, assuming humidity gradients would create an upward curvature of the slab (continuous higher moisture content at the bottom of the slab than at its surface) at any time of the day. At daytime, the effect of both the temperature and the humidity would produce a downward and an upward curvature respectively counteracting one another and producing thus, little vertical displacement as seen at 14:30 on Figure 6. On the other hand, at nighttime, both effects would produce and upward curvature which would add up and explain the significant difference between vertical displacements obtained from field and FE computations.

In Figure 6, the maximal vertical difference computed with field data are represented by red crosses and the magnitude of the linear temperature gradients, associated to those displacements, are presented with their respective extrapolated value after the arrow. For the largest maximal values of the vertical displacements difference of approximately 5 mm (early in the morning and producing an upward curvature), the only way to reproduce the effect of the humidity gradients is to introduce in the FE package an *Equivalent Temperature Gradient* (*ETG*). For both maximal values presented in Figure 6, negative gradients of twice the extrapolated magnitude would be required to predict the *in-field* displacement of the slab, i.e. with ΔT = - 8.7°C x 2 = -17.4°C a vertical displacement difference of around 5 mm is obtained. In the case of the positive gradients (daytime/downward curvature) the extrapolated thermal gradients (ΔT = +19.7°C) used in the FE package predict adequately the response of the slab in terms of vertical displacement difference despite their *non-linear* gradient distribution nature (see Figure 3b) and the presence of humidity gradients. Consequently, given the similar magnitude of both positive and negative gradients, an *ETG* of 17.4°C / 206 mm of slab thickness approximately equal to 0.08°C/mm will be used subsequently as a way to account for the effect of temperature and humidity in EverFE2.25. However, this *ETG* represents only the moments of the day where the maximal values occur as depicted in Figure 6.

3.4 Analysis of a typical JPCP section

In this section, the importance of considering temperature gradients when designing rigid pavements is demonstrated by simulating the behavior of a typical JPCP highway subject to vehicle and temperature (calibrated for the region under study) loading during the most critical moments of the day. The geometry and the

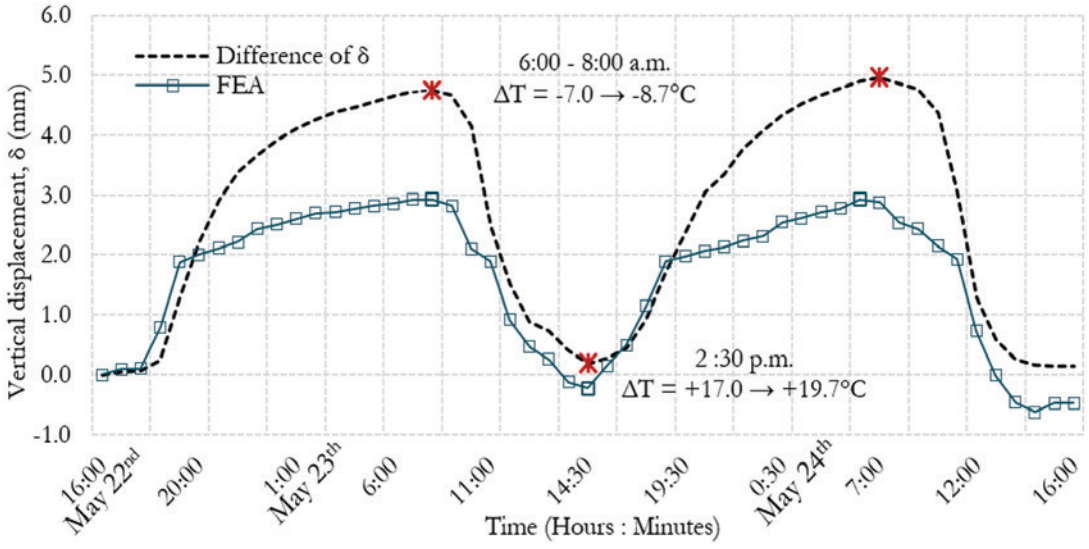

Figure 6
Vertical displacement of the slab based on FE analysis and *in-situ* measurements

material properties of the JPCP section are specified in Table 2. The section consists of two lanes (fast and slow) and a shoulder with 230 mm thick slabs. The concrete and the granular base properties are the same than those used in section 3.3. However, dowels (Ø = 32 mm) and ties (Ø = 12.7 mm) are used in the transversal and longitudinal joints respectively. In both cases, a load transfer efficiency of 70% [14] is assumed in accordance with the used value of their support moduli. The restraint moduli indicates the degree of bond between steel and concrete and thus, no bond is considered for dowels and the value for the ties is set to the default value used in EverFE2.25. The material properties of the dowels and the ties are also those proposed by default in EverfFE2.25. Load transfer efficiency between slabs by aggregate interlock is not considered since it is easily damaged after repeated medium to high traffic loading [15]. A 180 kN total weight dual wheel tandem axle is used as the vehicle load acting over the JPCP section. The axle's dimensions, as observed in Figure 7a, represent a common configuration of trailers. The print length of the wheel equal to 135 mm was calculated based on a fixed tire width of 220 mm and a pressure of 755 kPa (110 psi) [16].

The two most critical vehicle loading positions: *border* and *corner* as revealed by past research [2, 17] are studied here. In the *border* position (Figure 7b), the last dual tandem axle of the trailer is located 150 mm away from the longitudinal joint at the middle of the central slab. In the *corner* position (Figure 7c), the axle is positioned in the same transversal direction but 150 mm away from to the transverse joint of the central slab. With the geometry of the trailer, the second axle of the dual tandem truck axle would lay outside the JPCP geometry at the *border* position and the whole dual tandem axle would not be present when the truck would reach the *corner* position. However, only the central slab (blue dotted rectangle in Figure 7b and 7c) is of interest even though surrounding slabs were modeled. Indeed, their inclusion served only to recreate as accurately as possible the vertical displacement of the central slab due to the temperature (calibrated) and vehicle loading when the dowels and the ties restrain its vertical displacement.

The *Equivalent Temperature Gradients* (*ETG*) were chosen based on the results presented in section 3.3, i.e. an *ETG* of ±0.08°C/mm per slab thickness was used. This represents a somewhat conservative gradient for slabs thicker than 200 mm since gradients often increase disproportionally to their thickness [18]. By definition in this investigation, the *ETG* is assumed to vary linearly across the slab thickness based on the results presented in section 3.3. Thus, a gradient $\Delta T = \pm 18.5$°C is used for the 230 mm thick slab in combination with both vehicle loading positions.

The maximal principal stresses obtained from the analysis considering only the *ETG* (σ_{te}), the axle loads (σ_{ax}) and both at the same time (σ_{co}) are presented in Table 3. Stresses corresponding to σ_{te} and σ_{ax} are taken from the same location where the maximal stress resulting from their combined effect (σ_{co}) ocurrs; otherwise

Table 2
Properties of a typical JPCP highway section in Mexico

Category	Parameter	Value
Geometry	Fast lane length, l_h (mm)	4 500
	Slow lane length, l_s (mm)	3 500
	Shoulder length, l_{sh} (mm)	2 500
	Transverse joint spacing (mm)	4 500
	Slab thickness, h (mm)	230
Concrete	Young modulus, E (MPa)	26 500
	Poisson's ratio, ν	0.18
	C. of thermal expansion, α (/°C)	1.0×10^{-5}
	Density, γ (kg/m^3)	2 300
Base type	Winkler foundation	Tensionless
	k-value (MPa/mm)	0.28
Loading	Thermal gradient	Linear
	Vehicle	Border & Corner
Steel properties	Young modulus, E (MPa)	200 000
	Poisson ratio, ν	0.30
Dowels	Diameter, (mm)	32
	Length, (mm)	460
	Spacing, (mm)	300
	Support modulus, (MPa)	1 000
	Restraint modulus, (MPa)	0
Ties	Diameter, (mm)	12.7
	Length, (mm)	110
	Spacing, (mm)	900
	Support modulus, (MPa)	1 000
	Restraint modulus, (MPa)	10 000
Meshing	N° elements per slab	30 x 30 x 4

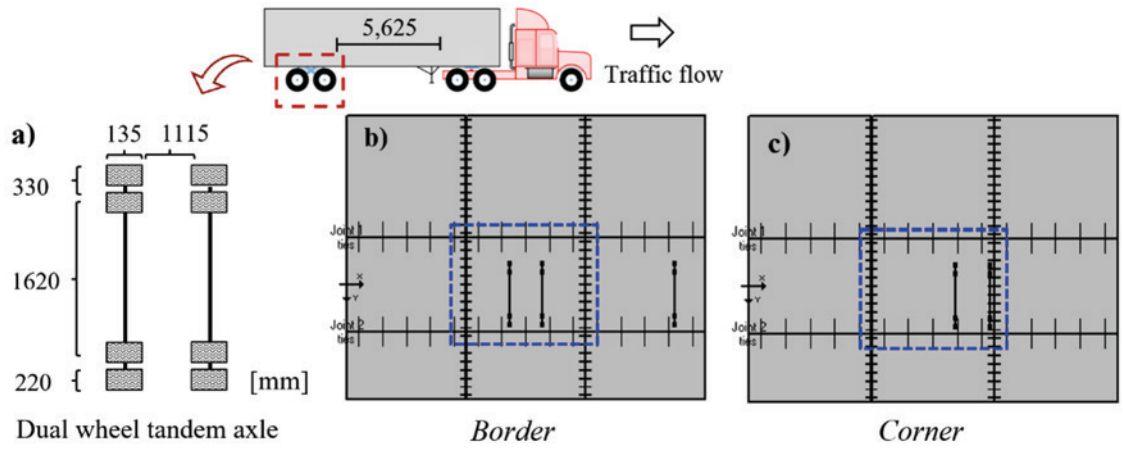

Figure 7
(a) Dual wheel tandem axle, (b) critical axle positions for positive gradient and (c) for negative gradients

Table 3
Maximal principal stresses for the two loading conditions

Position	ΔT* (°C)	σ_{te} (MPa)	σ_{ax} (MPa)	σ_{co} (MPa)	σ_{te} / σ_{ax}	(σ_{co} – σ_{ax}) / σ_{ax}	σ_{co} /M.O.R.**
Border	+18.5	1.42 (B)	0.74 (B)	3.17 (B)	1.9	3.3	0.70
	-18.5	1.54 (T)	0.32 (T)	2.09 (T)	4.8	5.5	0.46
Corner	+18.5	1.35 (B)	0.60 (B)	2.87 (B)	2.3	3.8	0.64
	-18.5	1.40 (T)	0.24 (T)	2.35 (T)	5.8	8.8	0.52

* Positive and negative temperature gradients create downward and upward slab curvature respectively;
** A M.O.R. of 4.5 MPa was considered.

the location would differ and comparisons would not be congruent. In addition, the surface where these stresses occur, either at the Bottom (B) or at the Top (T) of the slab, is indicated between parentheses in Table 3.

For both vehicle positions, the maximal σ_{co} stresses occur with a positive *ETG* and are developed at the bottom of the slab. These situations can be observed in Figure 8 for each vehicle loading position. As can be inferred from the results, the flexural strength of concrete specified for highway JPCPs (usually around 4.5 MPa of Modulus Of Rupture) can be reached when the temperature gradients are accounted in the analysis in addition to the vehicle loading. Here, slabs would fail under repeated loading for the most

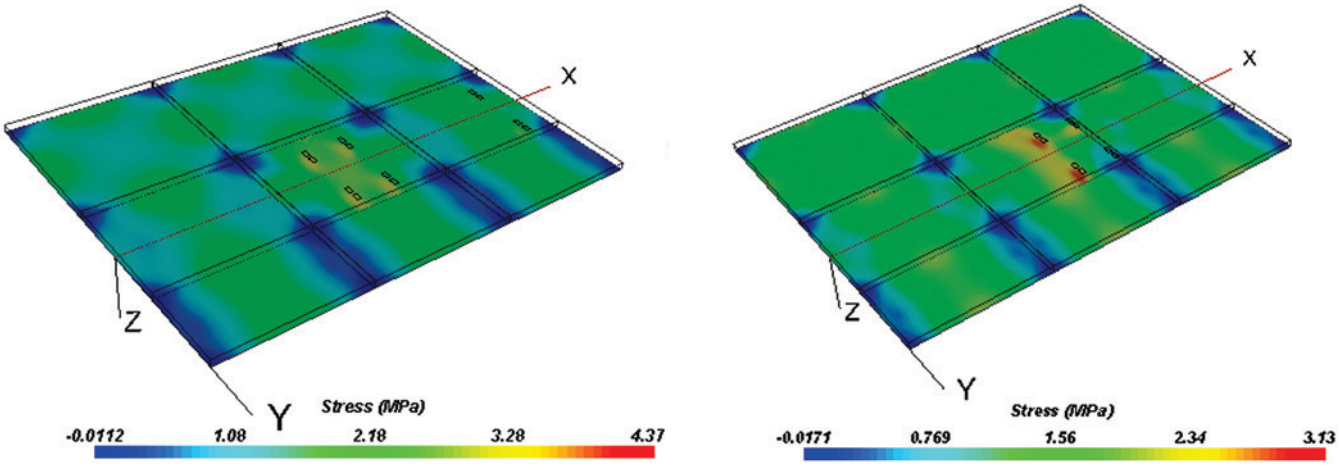

Positive gradient and *border* (B) **Positive gradient and *corner* (B)**

Figure 8
Maximal principal stresses for each combination of thermal and vehicle loads

critical loading conditions studied here since concrete pavements with ratios of σ_{co}/M.O.R. ≥ 0.5 are usually prone to fatigue failure. This situation would not have been noticed if the environmental loading using the *ETG* would not have been considered in the analysis.

The fact is that, the stresses induced by temperature (calibrated) gradients are, by themselves, considerably higher than those induced by the vehicle loads. In the case of the *border* position, they reached up to 4.8 times the axle load induced stress and in the *corner* position, up to 5.8 times when subject to a negative *ETG*. Furthermore, the apparent increase of the tensile stress attributable to the temperature gradient ($\sigma_{co} - \sigma_{ax}$) in comparison with the tensile stress induced by the axle is 5.5 times higher for the *border* position and as high as 8.8 times for the *corner* position. The considerable stress increase is due to the loss of the support of the slab at their center or corner depending on the sign of the temperature gradient. The actual stress state of slabs under heavier vehicle loads and their repetition would thus create situations in which failure would occur considerably faster.

4. Conclusions

The effect of local temperature gradients and vehicle loading on the performance of a JPCP was studied. Temperature gradients were measured in a test section in Guadalajara, Mexico and were then calibrated based on the vertical displacements calculated using a FE package in accordance to those measured *in-field*. A linear *Equivalent Temperature Gradient* of ±0.08°C/mm per slab thickness was found to be an adequate value to use in the region when analyzing a JPCP at the most critical moments of the day. A positive thermal gradient of such magnitude was indeed measured *in-situ* and when used as an input of the FE package, the vertical displacements of the test slab were adequately predicted. However, the *in-field* negative thermal gradient needed to be doubled to compensate for the *built-in* curling and the hypothesized humidity gradient acting in the slab during nighttime.

By using the *Equivalent Temperature Gradient* (as defined in this research for the most critical moments of the day) for the analysis of a typical JPCP highway section, it was shown that environmental loads represent a significant source of stresses by themselves, but mostly, when combined with vehicle loads. For the most critical loading combinations studied here (temperature and vehicle), it was shown that the apparent increase of the tensile stresses attributable to local temperature gradients can be as high as 5.5 times that of the standard axle studied here for the *border* position and up to 8.8 times for the *corner* position; both when negative gradients occur and for the slab geometry studied. Moreover, for the most critical loading condition, the stresses would surpass the commonly specified tensile strength of highways. Therefore, when designing JPCP *equivalent gradients* should be investigated and considered for each region to avoid premature crack formation and subsequent related problems such as pumping, and slab faulting [1, 18] which result in major repair costs. For similar climate conditions as Guadalajara, Mexico (monthly maximal and minimal average air temperature of +32.5°C and +9.5°C[3] respectively) a gradient of 0.08°C/mm may be considered. In other regions, the experimental campaigns designed to obtain temperature gradients should target the hottest seasons without rain to obtain the highest values of the gradients. Further research should investigate the relationship between air temperature variations and the temperature gradients for prediction purposes when larger data will be obtained for each region.

Moreover, in order to avoid as much as possible the initial loss of slab support during construction (*built-in* curling), which adds up to curling and warping, good construction practices cannot be overstated, i.e. timely and efficient curing in order to minimize water loss at the slabs surfaces. An interesting approach which has proved to be an effective way to maintain a constant humidity gradient across the slab thickness while the concrete hardens to avoid *built-in* curling [19] consists of internal curing of the slab using *water filled inclusions*. Sun and wind barriers to avoid rapid water surface evaporation should also be considered.

5. Acknowledgements

This article is dedicated to Prof. Marco Antonio Salcedo who worked arduously throughout the entire duration of the research project showing a lot passion and commitment. Special thanks are extended to the Faculty of Civil Engineering and Administration of the Panamerican University at the Guadalajara Campus, Mexico, for their funding support and to Dario Acosta and Rodrigo Navarro, deans of the faculty during the investigation, for their continuous support and encouragement.

6. References

[1] AASTHO. AASHTO Guide for Design of Pavement Structures, American Association of State Highway and Transportation Officials, 4ed, 1993, 595 p.

[2] PACKARD, R. G. Thickness Design for Concrete Highway and Street Pavements, Portland Cement Association, 1984, 46 p.

[3] CHOUBANE, B., TIA, M. Analysis and verification of thermal-gradient effects on concrete pavement. Journal of Transportation Engineering, v.121, n.1, 1995; p.75-81.

[4] CHOUBANE, B., TIA, M. Nonlinear temperature gradient effect on maximum warping stresses in rigid pavements. Transportation Research Record 1370, 1992; p.11-19.

[5] JEONG, J.-H., Zollinger, D. G. Environmental effects on the behavior of jointed plain concrete pavements. Journal of Transportation Engineering, v.131, n.2, 2005; p.140-148.

[6] SIDDIQUE, Z. Q., HOSSAIN, M., MEGGERS, D. Temperature and curling measurements on concrete pavement. Proceedings of the 2005 Mid-Continent Transportation Research Symposium, Iowa, 2005, 12 p.

[7] BELSHE, M. MAMLOUK, M. S., KALOUSH, K. E., RODEZNO M. Temperature gradient and curling stresses in concrete pavement with and without open-graded friction course. Journal of Transportation Engineering, v.137, n.10, 2011; p.723-729.

[3] *As of December 2010 from the National Meteorological Survey of Mexico.*

[8] HARR, M. E. Warping Stresses and Deflections in Concrete Slabs, Purdue University, 1958, 97 p.

[9] MOHAMED, A.R., HANSEN, W. Effect of nonlinear temperature gradients on curling stresses in concrete pavements, Transportation Research Record, n.1568, 1997; p.65-71.

[10] TIEDE, H., SPARLING, C., SMITH, P., PHANG, W. A. The Conditions of Concrete Pavements in Ontario, Department of highways Ontario, 1970, 30 p.

[11] CEYLAN, H., TURNER, D. J., RASMUSSEN, R. O., CHANG, G. K., GROVE, J., KIM, S., GOPALAKRISHNAN, K. Impact of Curling, Warping and Other Early-Age Behavior on Concrete Pavement Smoothness: Early, Frequent, and Detailed (EFD) Study, Iowa State University, 2007, 404 p.

[12] BASSO, T. P. Influence of the Temperature on the Behaviour of Rigid Pavements in Guadalajara, Bachelor's thesis (in Spanish), 2014, 177 p.

[13] ACI Committee 318. Building Code Requirements for Structural Concrete (ACI 318-14) and Commentary, American Concrete Institute, 2014, 519 p.

[14] DAVIDS, W. G. EverFe Theory Manual, University of Maine, 2003, 18 p.

[15] FHWA. Concrete Pavement Joints – Technical Advisory T5040.30, Federal Highway Administration, 1990, http://www.fhwa.dot.gov/pavement/t504030.cfm (consulted on November 2016).

[16] HUANG, Y. H. Pavement Analysis and Design, Pearson Prentice Hall, 2ed, 2004, 767 p.

[17] CHOU, Y. T. Comparative analysis of rigid pavements. Journal of Transportation Engineering, v.109, n.5, 1983; p.669-688.

[18] MTC. Pavement Condition Index Distress Identification Manual, Metropolitan Transportation Commission, 1991, 23 p.

[19] BENTZ, D. P. WEISS, W. J. Internal Curing: A 2010 State-Of-The-Art Review, National Institute of Standards and Technology, 2011, 82 p.